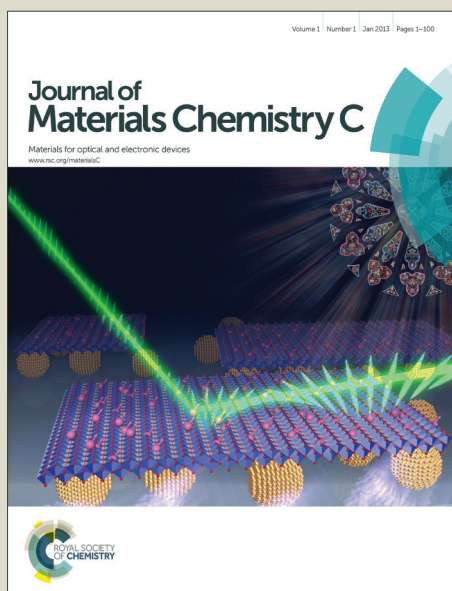


Journal of Materials Chemistry C

Accepted Manuscript



This is an *Accepted Manuscript*, which has been through the Royal Society of Chemistry peer review process and has been accepted for publication.

Accepted Manuscripts are published online shortly after acceptance, before technical editing, formatting and proof reading. Using this free service, authors can make their results available to the community, in citable form, before we publish the edited article. We will replace this *Accepted Manuscript* with the edited and formatted *Advance Article* as soon as it is available.

You can find more information about *Accepted Manuscripts* in the [Information for Authors](#).

Please note that technical editing may introduce minor changes to the text and/or graphics, which may alter content. The journal's standard [Terms & Conditions](#) and the [Ethical guidelines](#) still apply. In no event shall the Royal Society of Chemistry be held responsible for any errors or omissions in this *Accepted Manuscript* or any consequences arising from the use of any information it contains.

On-surface assembly of low-dimensional Pb-coordinated metal-organic structures

Cite this: DOI: 10.1039/x0xx00000x

Guoqing Lyu,^a Ran Zhang,^a Xin Zhang,^b Pei Nian, Liu^{b*} and Nian Lin^{a*}

Received 00th January 2012,
Accepted 00th January 2012

DOI: 10.1039/x0xx00000x

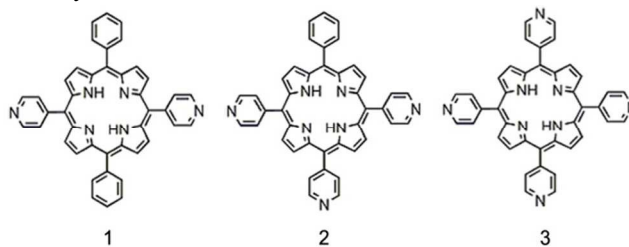
www.rsc.org/

Novel low-dimensional metal-organic structures incorporating heavy metal Pb atoms as coordination centres are formed on a Au(111) surface by means of on-surface metallo-supramolecular assembly. The molecular building blocks are porphyrin derivatives functionalized with pyridyl groups. These building blocks are linked via a unique pyridyl-Pb-pyridyl coordination motif that does not exist in conventional coordination chemistry but emerges on the surface. The specific sites of the pyridyl functions in the building blocks result in structures exhibiting distinctive morphologies, including one-dimensional single chains, double-chains and ladders, and two-dimensional porous networks.

Introduction

Metal-organic frameworks (MOFs) incorporating *p*-block metals are very rare in contrast to the abundantly-reported *d*- or *f*-block metal coordinated MOFs. Pb, as a heavy *p*-block element, has a large radius, versatile stereochemical activities and a flexible coordination environment.¹⁻³ These characteristics provide opportunities for constructing Pb-based MOFs that exhibit rich structural topologies and diverse coordination geometries.⁴⁻¹¹ Moreover, the unique electronic configuration of Pb makes the Pb-based MOFs potential electroluminescent devices, light-emitting diode and fluorescent sensors.⁹⁻¹¹ Recently, it was demonstrated theoretically that a Pb-based two-dimensional (2D) organometallic structure exhibits a non-trivial quantum state, known as topological insulator phase, caused by the strong spin-orbit coupling effects of the heavy Pb atoms.¹² This prediction hints that the Pb-coordinated 2D metal-organic structures may represent a new family of functional materials with appealing electronic and spintronic properties. Experimental realization of these predicated structures is therefore highly desirable.

Supramolecular coordination self-assembly taking place at solid-vacuum interfaces is a powerful tool for designing 2D MOFs.¹³⁻¹⁶ Up to now, the 2D MOFs are mainly constructed with alkali, transition and rare earth, i.e., *s*-,¹⁷⁻²⁰ *d*-,²¹⁻²⁸ and *f*-block²⁹⁻³¹ metals, while the main group *p*-block metals remain unexplored. Here we report the self-assembly of Pb-coordinated metal-organic structures on a Au(111) surface. We used three pyridyl functionalized porphyrin derivatives (**Scheme 1**) as molecular building blocks to coordinate with Pb. We found that Pb is coordinated in a two-fold pyridyl-Pb-pyridyl motif, which resembles the previously-reported pyridyl-Cu-pyridyl bonding motif on the same surface.^{32, 33} We observed that Pb assemble with **1** to form single-row chains, with **2** to form double-row chains and ladders and with **3** to form two types of porous 2D networks exhibiting rhombus and Kagome lattices, and a multiple-row structure. To our knowledge, this is the first report of on-surface synthesized metal-organic structures based on Pb coordination. We also investigated the assembly pathway and thermal stability of these structures and found that the Pb-coordinated bonds are weaker than the Cu-coordinated counterparts, presumably due to its *p*-block chemistry.



Scheme 1 Chemical structures of the porphyrin derivatives used in this study: 5,15-dipyridyl-10,20-diphenylporphyrin (**1**); 5,10,15-tri(4-pyridyl)-20-phenylporphyrin (**2**) and 5,10,15,20-tetra(4-pyridyl)-porphyrin (**3**).

Results and Discussion

Fig. 1 is an STM topograph showing mixture of **1** and Pb on the Au(111) surface. The molecules **1** were deposited first and Pb atoms deposited later on the sample. During the deposition, the sample was held at room temperature. Without Pb, molecules **1** were in a highly mobile 2D gas phase on the surface. The hexagonal-shaped islands in Fig. 1 are Pb islands. The molecules form two structures. Most molecules aggregated as closely-packed islands (blue arrow) and a small portion of the molecules form chains (white arrow). The up-left insert in Fig. 1 is a magnified image of the closely-packed molecule islands with a molecular model overlaid. This structure can be rationalized by inter-molecular hydrogen bonds arising from the periphery pyridyl functions, as highlighted by the dashed lines in the model (see detail description and discussion in the ESI).

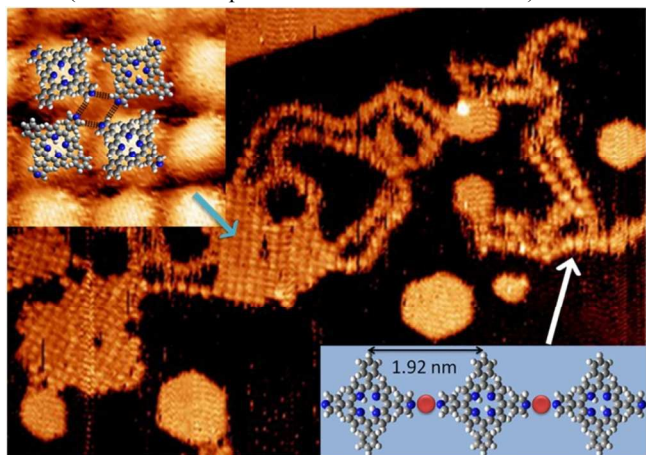


Fig. 1 (a) An overview STM topograph showing **1** and Pb form SR chains ($100 \times 70 \text{ nm}^2$). Up-left inset: magnified view of a closely-packed network ($4 \times 4 \text{ nm}^2$) with a tentative model overlaid. The dashed lines indicate hydrogen bonds. Bottom-right inset: Structural model of the SR chain. Color code: C, gray; N, blue; H, white; Pb, red.

The chains are composed of single-row of molecules, denoted as SR chains thereafter. Note that the SR chains often terminate at a Pb island or a molecule island. Many SR chains are not perfect straight but exhibit a curved morphology. The SR chains frequently changed their morphology during STM scanning, indicating the SR chains were mobile. These phenomena reflect that the inter-molecular bonding in the SR chains is flexible. The distance between the neighboring molecules in the SR chains is $1.92 \pm 0.05 \text{ nm}$. Similar chain structures were observed in self-assembly of **1** and Cu on Au(111) and were confirmed to be metal-organic chains with a pyridyl-Cu-pyridyl bonding motif.³³ We attribute the SR chains to a similar structure that is stabilized by two-fold pyridyl-Pb-pyridyl coordination, as illustrated in the structural model in the bottom-right inset in Fig. 1. Despite their distinctive bonding configuration in three-dimensional space, Cu and Pb may be coordinated in similar bonding motifs on a surface, suggesting the surface alters the intrinsic properties of the adsorbed metal atoms. Assuming that the Pb atom locates at the middle of the two N atoms of the opposing pyridyl groups, the Pb-N bond length is estimated to be $0.20 \pm 0.02 \text{ nm}$. This length becomes larger if the Pb atom is not

co-planar with the two N atoms or the porphyrin molecules slightly rotate azimuthally. Pb(II) coordination with N-donor ligands such as 2,2'-bipyridine and 4,4'-bipyridine ligands have been reported in solution phase complexes,³⁴⁻³⁶ which feature a Pb-N bond length in the range of 0.24 to 0.26 nm. The bond length of the on-surface Pb-N coordination thus is comparable with the typical Pb-N bond length in the solution phase complexes.

Annealing the sample to $100 \text{ }^\circ\text{C} \sim 150 \text{ }^\circ\text{C}$ reduced the amounts of SR chains and shortened their length, in the mean time increased the size of the closely-packed molecule islands. Annealing the sample above $150 \text{ }^\circ\text{C}$ caused the SR chains to disappear entirely and all molecules aggregated as molecule islands while Pb atoms form big Pb islands. These phenomena indicate that the SR chains are kinetically-controlled products. Presumably, the on-surface pyridyl-Pb-pyridyl coordination is of moderate bond strength so that the free energy of the SR chains is higher than that of a system consisting of the closely-packed molecule islands and the Pb islands.

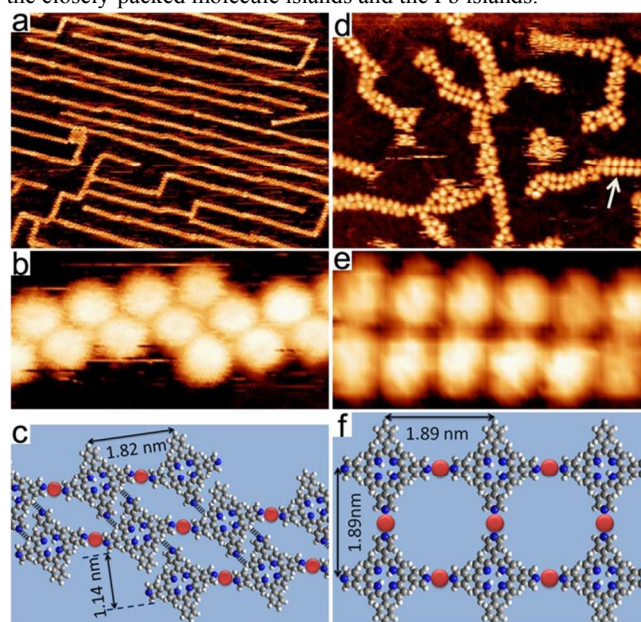


Fig. 2 (a) and (d) STM topographs showing DR chains and the ladder structures formed out of **2** and Pb ($113 \times 151 \text{ nm}^2$ and $54 \times 72 \text{ nm}^2$), respectively. (b) and (e) High-resolution images of a DR chain and a ladder structure ($5 \times 10 \text{ nm}^2$). (c) and (f) Structural models of the DR chain and the ladder structure, respectively. The dashed lines indicate hydrogen bonds.

Molecules **2** deposited on Au(111) were in a highly mobile 2D gas phase too. After dosing Pb atoms on this sample held at room temperature, closely-packed molecule islands appeared. Annealing the sample at $140 \text{ }^\circ\text{C}$ induced the formation of line structures (Fig. 2a). The lines are very long, with some extending over 400 nm, and feature kinks, right-angle turns and T-shape joints (see the ESI). Fig. 2b is a magnified view of a line with a kink. The line is made out of double rows of molecules (denoted as DR). Two neighboring rows are inter-locked in a zigzag manner with a row-to-row distance of $1.14 \pm 0.05 \text{ nm}$. A structural model of the DR structure is shown in Fig. 2c: the molecules are linked via pyridyl-Pb-pyridyl coordination along the rows. Along the row axes, the neighboring molecules are 1.82-nm apart, which is 0.1 nm closer than those in an SR chain. To

attain a reasonable Pb-N distance, we propose that the molecules in the **DR** chains turn azimuthally. As the model (Fig. 2c) shows, the molecules rotate 8° off the long axes of the row, resulting in a 0.20 ± 0.02 nm Pb-N distance. The model also shows that the N atom of the ortho-pyridyl group approaches the H atom at a *beta*-position of the porphyrin moiety of the molecule in the adjacent row. The N-H distance is 0.20 ± 0.02 nm (dashed line), which may invoke an intermolecular hydrogen bond. Such hydrogen bonds inter-link two rows into the **DR** structure. At the kink, a molecule flips upside down to form hydrogen bonds with the molecule(s) in the upper row and the molecule(s) in the down row. One possible scenario is illustrated in Fig. 2c.

Dosing additional amount of Pb on this sample and annealing at 170°C formed a ladder structure (Fig. 2d, white arrow) along with the **DR** chains. The ladders are shorter than the **DR** chains, typically consisting of less than 10 dimer units. As shown in a high-resolution STM image of a ladder (Fig. 2e), each molecule links to three neighboring ones at a distance of 1.89 ± 0.05 nm. We proposed that in this structure all three pyridyl groups participate in pyridyl-Pb-pyridyl coordination (Fig. 2f).³⁷ The ladder structures are less stable than the **DR** chains, as evidenced by the structural changes occurred during STM scanning. Moreover, after annealing the sample at 200°C , the ladders disappeared but the **DR** chains remained. The thermal stability of the **DR** and ladder structures will be discussed later.

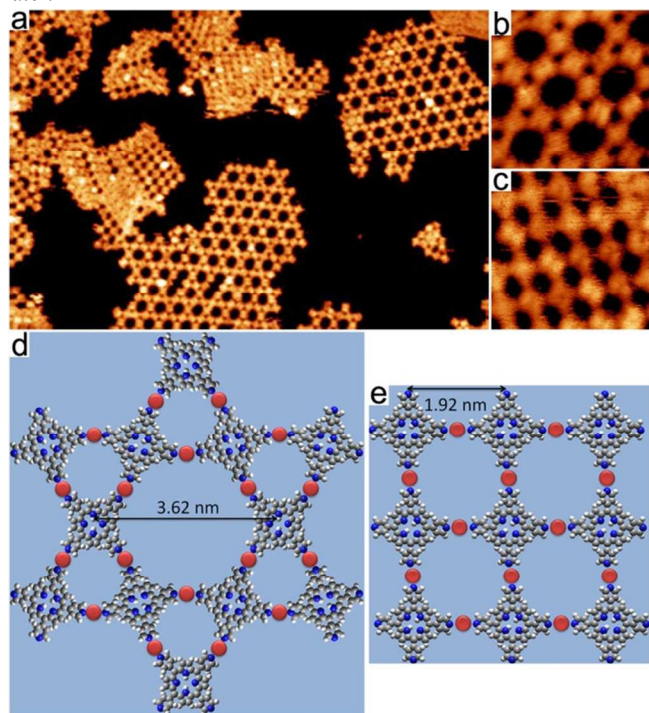


Fig. 3 (a) STM topograph showing **3** and Pb form close-packed islands, Kagome and rhombus porous networks (90×60 nm²). (b) and (c) High-resolution images of the Kagome and rhombus networks (12×12 nm²). (d) and (e) Structural models of the Kagome and rhombus networks.

Depositing Pb first and molecules **3** later, or simultaneous deposition of the two components, on the Au(111) generated closely-packed molecule islands and Pb islands, but no coordination structures (see the ESI). To form well-ordered coordination

structures, molecules **3** were deposited on the surface first, Pb atoms were deposited later onto the sample which was held at 60 - 120°C . Fig. 3a displays that two types of porous networks appeared, exhibiting a Kagome lattice and a rhombus lattice, respectively, along with small patches of closely-packed molecule islands. The Kagome networks grew on open terraces with a typical domain size of 30 nm \sim 50 nm. The rhombus networks are smaller, with a typical domain size below 20 nm, and always connected with the closely-packed molecule islands. Fig. 3b is a high resolution STM image of the Kagome structure. One can see that each molecule is attached to four neighboring ones, whereas three molecules form a symmetric three-branch joint, thus constructing a Kagome lattice.²⁶ The diameter of the hexagon is 3.63 ± 0.05 nm. Fig. 3d shows a model of the Kagome structure with a Pb-N distance of 0.20 ± 0.02 nm. Fig. 3c is a high-resolution STM image of the rhombus structure. The rhombus has two corners at 85° and two corners at 95° . This deviation from a perfect square structure is attributed to the symmetry mismatch between the network and the substrate.^{38, 39} The side of the rhombus structure is 1.92 ± 0.05 nm long, featuring a Pb-N bond length of 0.20 ± 0.02 nm. Fig. 3e is a model of the rhombus structure.

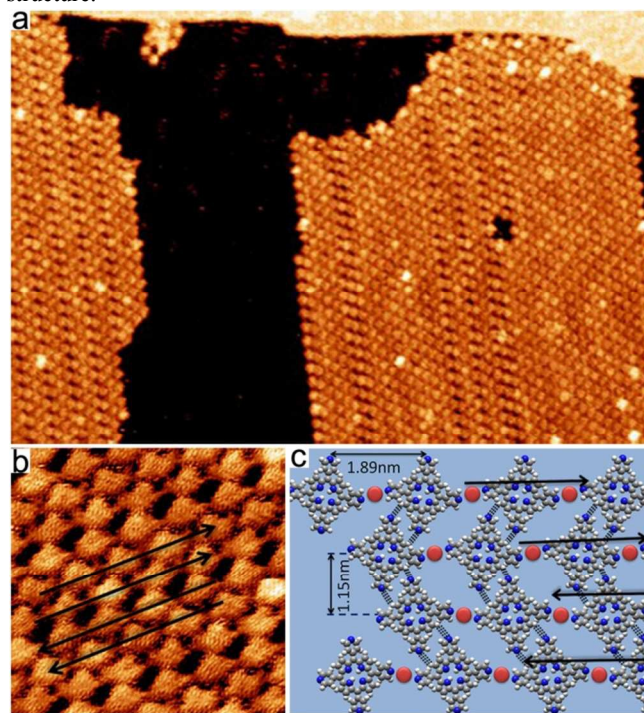


Fig. 4 (a) An overview STM topograph of **MR** structure (90×60 nm²). (b) High-resolution image (10 nm \times 10 nm²). The arrows highlight the rows. (c) Structural model of the **MR** structure. The dashed lines indicate hydrogen bonds. The arrow direction indicates the azimuth rotation of the molecules in that row.

Annealing this sample at 160°C destroyed both porous network structures and formed a new structure. As shown in Fig. 4a, molecules **3** formed 2D islands as large as ~ 100 nm. The islands always ended at mono-atomic steps of the Au(111) surface and have two straight edges, implying that the inter-molecular interaction is different along the two orthogonal directions in the islands. Close inspection revealed that the islands contain rows of holes. A magnified STM topograph (Fig. 4b) shows that the 2D island

consists of multiple parallel molecule rows (denoted as **MR**), as highlighted with the black arrow lines. Along the rows, the molecules arrange with an inter-molecular distance of 1.89 ± 0.05 nm. The adjacent rows are packed with a row-to-row distance of 1.15 ± 0.05 nm. This structure thus is similar as the **DR** structure. We propose that the bonding configuration in the **MR** structure resembles the **DR** chains, that is, pyridyl-Pb-pyridyl coordination along each row and hydrogen bonding between the adjacent rows, as illustrated in the structural model in Fig. 4c. The arrows define the clockwise or counter clockwise azimuth rotation of the molecules with respect to the row axes. As the two adjacent rows are made out of opposite rotated molecules, larger voids appear between the two rows, accounting for the holes in the STM topograph.

The six Pb-coordinated structures were assembled at specific conditions and exhibited different thermal stability, as summarized in Table 1. To form the **SR** structure, molecules **1** were first deposited on the surface and subsequently Pb atoms were dosed at the room-temperature sample. Reversing the deposition sequence or simultaneous deposition of the two components did not result in the **SR** structure. Annealing the sample at 150°C and cooling to 30°C dissolved the **SR** structure. This behaviour hints that the self-assembly of the **SR** structure is a kinetically-controlled process. In contrast, self-assembly of the **DR** structure required high-temperature annealing of the mixture of molecules **2** and Pb atoms, so this process is thermodynamically controlled. The ladder structure, however, formed at a moderate annealing temperature of 170°C and dissolved after 200°C annealing. Thus the assembly of the ladder structure is a process ruled by both kinetic and thermodynamic controls. The self-assembly of the porous networks is most intriguing. It took place at the conditions of (1) molecules **3** must be deposited on the surface first; (2) Pb atoms were dosed to the sample which was held at $60\text{-}120^\circ\text{C}$; (3) the dosing flux of Pb was kept very low, $0.02\text{ML}/\text{minute}$. Deviation from these optimized conditions reduced network size and more molecules were incorporated in the closely-packed molecule islands. Moreover, annealing treatments did not enlarge but rather reduced the network domain size. The porous networks were dissolved with 160°C annealing, thus, are kinetic products. The **MR** structure, in contrast, remained stable even after 240°C annealing. Apparently, this structure is a thermodynamic product. Note that among the five

structures, two thermodynamic products of the **DR** and **MR** structures can be assembled by dissolving Pb islands with high-temperature annealing in the presence of the corresponding molecules.

The differences in the self-assembly behaviours and thermal stability can be partially rationalized in terms of inter-molecular bond energy. The number of bonds per molecule in each structure is listed in Table 1. Among the five structures, those stabilized purely by coordination bonds are kinetically-controlled structures, while those stabilized by a combination of coordination and hydrogen bonds are the thermodynamic stable ones. The **MR** structure, which has two coordination bonds and two hydrogen bonds per molecule, is more stable than the porous network structures which have four coordination bonds per molecule. Likewise, the **DR** structure, which has two coordination bonds and one hydrogen bond per molecule, is more stable than the ladder structure which has three coordination bonds per molecule. We propose that the surface-stabilized pyridyl-Pb-pyridyl coordination is of moderate strength, which is comparable or even weaker than the inter-molecular hydrogen bonds. Therefore the thermal stability of these structures can be correlated with the average bond energy per molecule.

Conclusions

In summary, we have investigated the self-assembly of Pb with a series of pyridyl-functionalized porphyrin derivatives. A two-fold pyridyl-Pb-pyridyl coordination motif articulates the molecular building blocks into metal-organic structures. The number and positions of the pyridyl groups on the porphyrin molecules control the dimensionality of the metal-organic structures, ranging from one-dimensional (single-row chains), quasi 2D (ladders) to 2D (porous networks). The structures involving coordination bonds only are metastable kinetic products, whereas the structures involving a combined coordination and hydrogen bonds are thermodynamic products. These features imply that the *p*-block chemistry of Pb results in relative weak pyridyl-Pb-pyridyl coordination as compared with those incorporating *d*-block elements. The physical and chemical properties of these structures including the oxidation state of the Pb atoms deserve further studies. The structures reported here are in close contact with the Au surface, which might significantly alter their electronic, in particular the non-trivial topological,

Table 1. Summary of the structures formed in this study and their assembly conditions.

* C stands for coordination bond and H hydrogen bond.

** As the Kagome and the rhombus networks exhibit similar self-assembly and structural characteristics, these two structures are categorized as porous networks and represented by the model of a square network.

Molecule	1	2	3		
Structure	SR	DR	Ladder	Porous Networks**	MR
Deposition sequence	1) 1 ; 2) Pb	Arbitrary	Arbitrary	1) 1 ; 2) Pb	Arbitrary
Assembly Temperature	$30\text{-}100^\circ\text{C}$	$140\text{-}180^\circ\text{C}$	170°C	$60\text{-}120^\circ\text{C}$	$200\text{-}240^\circ\text{C}$
Assembly Path	Kinetic	Thermodynamic	Kinetic	Kinetic	Thermodynamic
Thermal Stability	low	high	moderate	moderate	highest
Model					
No. bonds* per molecule	2 C	2 C + 1 H	3 C	4 C	2C+2 H

properties. To realize the structures that resemble the free-standing 2D organic topological insulating layers presented in Ref. 12, it is highly desirable to form these structures on an insulating substrate.

Experimental Section

All the experiments were conducted in an ultrahigh-vacuum system (Omicron Nanotechnology) with a base pressure of 3×10^{-10} mbar. A single-crystalline Au(111) substrate was cleaned by repeated cycles of Ar⁺ sputtering and annealing to about 620 °C afterwards. The molecules **1**, **2**, and **3** were evaporated at 320 °C, 340 °C, and 355 °C, respectively, and deposited onto the Au(111) surface held at room temperature. Pb atoms were dosed onto the Au(111) surface by an electron-beam evaporator. The samples were characterized by a scanning tunneling microscope operated at room temperature in a constant current mode with tunnelling current of 0.5 nA and bias voltage 1.5 V. **1** and **2** were synthesized³⁷ and **3** was purchased from Sigma Aldrich.

Acknowledgement

This work is supported by Hong Kong RGC 603213, the National Natural Science Foundation of China (Project Nos. 21172069, 21372072 and 21190033) and the Science Fund for Creative Research Groups (21421004).

Notes and references

^a Department of Physics, The Hong Kong University of Science and Technology, Clear Water Bay, Hong Kong, China. E-mail: phnlin@ust.hk

^b Shanghai Key Laboratory of Functional Materials Chemistry and Institute of Fine Chemicals, East China University of Science and Technology, Meilong Road 130, Shanghai, China. E-mail: liupn@ecust.edu.cn

- P. Pyykk, *Chem. Rev.* 1988, **88**, 563-594.
- J. M. Harrowfield, H. Miyamae, B. W. Skelton, A. A. Souidi, A. H. White, *Aust. J. Chem.* 1996, **49**, 1165-1169.
- L. Shimoni-Livny, J. P. Glusker, C. W. Brock, *Inorg. Chem.* 1998, **37**, 1853-1867.
- E.C. Yang, J. Li, B. Ding, Q.Q. Liang, X.G. Wang, X.J. Zhao, *CrystEngComm*, 2008, **10**, 158-161.
- S.R. Fan, L.G. Zhu, *Inorg. Chem.* 2006, **45**, 7935-7942.
- B. J. Greer, V. K. Michaelis, M. J. Katz, D. B. Leznoff, G. Schreckenbach, S. Kroeker, *Chemistry*. 2011, **17**, 3609-3618.
- L. Zhang, Z.-J. Li, Q.-P. Lin, Y.-Y. Qin, J. Zhang, P.-X. Yin, J.-K. Cheng, Y.-G. Yao, *Inorg. Chem.* 2009, **48**, 6517-6525.
- J. Yang, J.-F. Ma, Y.-Y. Liu, J.-C. Ma, S. R. Batten, *Inorg. Chem.* 2007, **46**, 6542-6555.
- B. Sui, W. Zhao, G. Ma, T. Okamura, J. Fan, Y. Z. Li, S. H. Tang, W. Y. Sun, N. Ueyama, *J. Mater. Chem.* 2004, **14**, 1631-1639.
- J. E. H. Buston, T. D. W. Claridge, S. J. Heyes, M. A. Leech, M. G. Moloney, K. Prout, *Dalton Trans.* 2005, 3195-3203.
- J.-G. Mao, Z.-K. Wang, A. Clearfield, *Inorg. Chem.* 2002, **41**, 6106-6111.
- Z. F. Wang, Z. Liu, F. Liu, *Nature Commun.* 2013, **4**, 1471.
- J. V. Barth, *Annu. Rev. Phys. Chem.* 2007, **58**, 375-407.
- S. Stepanow, N. Lin, J. V. Barth, *J. Phys.: Condens. Matter* 2008, **20**, 184002.
- N. Lin, S. Stepanow, M. Ruben, J. V. Barth, *Top. Curr. Chem.* 2009, **287**, 1-44.
- H. Liang, Y. He, Y. Ye; X. Xu, F. Cheng, W. Sun, X. Shao, Y. Wang, J. Li, K. Wu, *Coord. Chem. Rev.* 2009, **253**, 2959-2979.
- S.; Stepanow, R. Ohmann, F. Leroy, N. Lin, T. Strunskus, Ch. Wöll, K. Kern, *ACS Nano* 2010, **4**, 1813-1820.
- C. Wäckerlin, C. Iacovita, D. Chylarecka, P. Fesser, T. A. Jung, N. Ballav, *Chem. Commun.* 2011, **47**, 9146-1820.
- D. Skomski, S. Abb, S. L. Tait, *J. Am. Chem. Soc.* 2012, **134**, 14165-14171.
- N. Abdurakhmanova, A. Floris, T.-C. Tseng, A. Comisso, S. Stepanow, A. De Vita, K. Kern, *Nature Commun.* 2012, **3**, 940.
- A. Dmitriev, H. Spillmann, N. Lin, J. V. Barth, K. Kern, *Angew. Chem. Int. Ed.* 2003, **42**, 2670-2673.
- S. Stepanow, N. Lin, D. Payer, U. Schlickum, F. Klappenberger, G. Zoppellaro, M. Ruben, H. Brune, J.V. Barth, K. Kern, *Angew. Chem. Int. Ed.* 2007, **46**, 710-713.
- S. L. Tait, A. Langner, N. Lin, R. Chandrasekar, M. Ruben, K. Kern, *ChemPhysChem*. 2008, **9**, 2495-2499.
- T.-C. Tseng, C. Lin, X. Shi, S. L. Tait, X. Liu, U. Starke, N. Lin, R. Zhang, C. Minot, M. A. Van Hove, J. I. Cerdá, K. Kern, *Phys. Rev. B.* 2009, **80**, 155458.
- J. Čechal, Ch. S. Kley, T. Kumagai, F. Schramm, M. Ruben, S. Stepanow, K. Kern, *Chem. Commun.* 2014, **50**, 9973-9976.
- Z. Shi, N. Lin, *J. Am. Chem. Soc.* 2009, **131**, 5376-5377.
- D. Skomski, C. D. Tempas, G. S. Bukowski, K. A. Smith, S. L. Tait, *J. Chem. Phys.* 2015, **142**, 101913.
- D. Skomski, C. D. Tempas, K. A. Smith, S. L. Tait, *J. Am. Chem. Soc.* 2014, **136**, 9862-9865.
- J. I. Urgel, D. Ecija, W. Auwärter, A. C. Papageorgiou, A. P. Seitsonen, S. Vijayaraghavan, S. Joshi, S. Fischer, J. Reichert, J. V. Barth, *J. Phys. Chem. C.* 2014, **118**, 12908-12915.
- J. I. Urgel, D. Ecija, W. Auwärter, J. V. Barth, *Nano Lett.* 2014, **14**, 1369-1373.
- D. Ecija, J. I. Urgel, A. C. Papageorgiou, S. Joshi, W. Auwärter, A. P. Seitsonen, S. Klyatskaya, M. Ruben, S. Fischer, S. Vijayaraghavan, J. Reichert, J. V. Barth, *Proc. Natl. Acad. Sci. U.S.A.* 2013, **110**, 6678-6681.
- S. L. Tait, A. Langner, N. Lin, S. Stepanow, C. Rajadurai, M. Ruben, K. Kern, *J. Phys. Chem. C.* 2007, **111**, 10982-10987.
- T. Lin, X. S. Shang, J. Adisojojoso, P. N. Liu, N. Lin, *J. Am. Chem. Soc.* 2013, **135**, 3576-3582.
- A. Morsali, M. Payeghader, S. S. Monfared, M. Moradi, *J. Coord. Chem.* 2003, **56**, 761-770.
- A. Morsali, X.-M. Chen, *J. Coord. Chem.* 2004, **57**, 1233-1241.
- K. J. Nordell, K. N. Schultz, K. A. Higgins, M. D. Smith, *Polyhedron* 2004, **23**, 2161-2167.
- J. Adisojojoso, Y. Li, J. Liu, P. N. Liu, N. Lin, *J. Am. Chem. Soc.* 2012, **134**, 18526-18529.
- Z. Shi, N. Lin, *ChemPhysChem*. 2010, **11**, 97-100.
- Y. Li, J. Xiao, T. Shubina, M. Chen, Z. Shi, M. Schmid, H-P. Steinrueck, M. Gottfried, N. Lin, *J. Am. Chem. Soc.* 2012, **134**, 6401-6408.

Table of Contents:

On-surface assembly of low-dimensional Pb-coordinated metal-organic structures

Guoqing Lyu,^a Ran Zhang,^a Xin Zhang,^b Pei Nian, Liu^{b*} and Nian Lin^{a*}

^a Department of Physics, The Hong Kong University of Science and Technology, Clear Water Bay, Hong Kong, China.

^b Shanghai Key Laboratory of Functional Materials Chemistry and Institute of Fine Chemicals, East China University of Science and Technology, Meilong Road 130, Shanghai, China.

Porphyrin-based one-dimensional chains, ladders, and two-dimensional networks incorporating *p*-block element Pb are assembled on a Au(111) surface.

